

Redox-mediated Effects of Selenium on Apoptosis and Cell Cycle in the LNCaP Human Prostate Cancer Cell Line¹

Weixiong Zhong and Terry D. Oberley²

Department of Pathology and Laboratory Medicine, University of Wisconsin Medical School, Madison, Wisconsin 53706 [W. Z., T. D. O.], and Pathology Service, William S. Middleton Memorial Veterans Hospital, Madison, Wisconsin 53705 [T. D. O.]

ABSTRACT

The effects of selenium exposure were studied in LNCaP human prostate cancer cells, and this same cell line adapted to selenium over 6 months to compare acute *versus* chronic effects of sodium selenite, the latter most closely resembling human clinical trials on the effects of selenium in cancer prevention and therapy. Our results demonstrated that oxidative stress was induced by sodium selenite at high concentrations in both acute and chronic treatments, but outcomes were different. After acute exposure to selenite, cells exhibited mitochondrial injury and cell death, mainly apoptosis. After chronic exposure to selenite, cells showed growth inhibition caused by cell cycle arrest, increased numbers of mitochondria and levels of mitochondrial enzymes, and only minimal induction of apoptosis. Immunoblotting analysis revealed that multiple proteins were up-regulated by chronic exposure to selenite. Among them, only up-regulation of manganese superoxide dismutase and the cyclin-dependent kinase inhibitor p21^{Waf1/Cip1}, proteins known to be redox sensitive and to have cell cycle regulatory functions, correlated with cell growth inhibition. Our results in selenite-adapted cells suggest that selenium may exert its effects in human prostate cancer cells by altering intracellular redox state, which subsequently results in cell cycle block.

INTRODUCTION

Selenium, an essential nutritional trace element, has been known to be an essential component in the enzymatic active site of GPX,³ one of the key enzymes involved in detoxification of hydrogen peroxide (1). Recent studies have demonstrated that selenium is also an essential element of Trx Rs of the Trx redox system, which has been shown to have multiple functions, including regulating cell growth and apoptosis (2, 3). In addition, selenium compounds have been demonstrated to have antitumorogenic activities in animal models by inhibiting tumor initiation and promotion (4). Selenium compounds inhibit the growth of a variety of tumor cells *in vitro* via the induction of apoptosis (5–7). Epidemiological studies have suggested that low serum selenium levels were associated with an increase in the incidence of cancer (8–10). Recent clinical trials showed that supplemental selenium reduced the incidence and mortality of at least five types of human cancers, including prostate cancer (11–13). A recent epidemiological study also showed that high levels of toenail selenium were associated with lower incidence and slower progression of human prostate cancer (14).

Received 3/6/01; accepted 8/2/01.

The costs of publication of this article were defrayed in part by the payment of page charges. This article must therefore be hereby marked *advertisement* in accordance with 18 U.S.C. Section 1734 solely to indicate this fact.

¹ Supported by the Veterans Administration Research Service (to T. D. O.) and the Department of Pathology and Laboratory Medicine (to W. Z.), University of Wisconsin Medical School.

² To whom requests for reprints should be addressed, at Pathology and Laboratory Medicine Service, Room A35, William S. Middleton Memorial Veterans Administration Hospital, 2500 Overlook Terrace, Madison, WI 53705. Phone: (608) 256-1901, extension 11722; Fax: (608) 280-7087; E-mail: toberley@facstaff.wisc.edu.

³ The abbreviations used are: GPX, glutathione peroxidase; BSO, buthionine sulfoximine; CuZnSOD, copper and zinc-containing superoxide dismutase; GSH, reduced glutathione; GSSG, oxidized glutathione; MnSOD, manganese-containing superoxide dismutase; MnTMPyP, manganese (III) tetrakis (1-methyl-4-pyridyl) porphyrin pentachloride; MTT, 3-[4,5-dimethylthiazol-2-yl]-2,5-diphenyl-tetrazolium bromide; NAC, N-acetylcysteine; ROS, reactive oxygen species; SOD, superoxide dismutase; Trx, thioredoxin; Trx Px, peroxiredoxin; Trx R, thioredoxin reductase; TTBS, Tween 20 Tris-buffered saline; CAT, catalase.

Prostate cancer is the most commonly diagnosed and second leading cause of cancer death in men in the United States (15). The etiology of prostate cancer remains unknown, and there are no effective chemopreventive and/or chemotherapeutic agents for prostate cancer. However, a recent clinical trial and an epidemiological study have shown that selenium is a promising chemopreventive agent for prostate cancer (11, 14). To date, there are only a few published studies on the *in vitro* effects of selenium on prostate cancer cell lines. These studies focused on acute short-term effects (6, 16–18). There is a scarcity of studies on the long-term effects of selenium in prostate cancer cells. Information on the effects of selenium on prostate cancer cells is important because studies of the effects of selenium on cancer prevention in humans are currently being conducted, and it is possible that a small number of human subjects could actually have early but clinically undetectable prostate cancer at the time of initiation of clinical trials. Thus, it is important to know what the long-term effects of selenium on these early cancers will be.

The chemopreventive and chemotherapeutic mechanisms of selenium remain unclear. Many potential mechanisms have been proposed, including protection against oxidative damage, modulation of metabolism of carcinogens, cytotoxicity of selenium metabolites, induction of apoptosis secondary to production of ROS, regulation of the Trx redox system, regulation of the cell cycle, and inhibition of angiogenesis (19–22). In addition, GSH and NADPH are consumed, and GSSG and NADP⁺ are produced during the redox metabolism of selenite (7, 19, 22). This may alter the intracellular redox state, which has been known to be crucial for a variety of biological functions, including regulation of gene expression.

ROS, mainly superoxide, hydrogen peroxide, and hydroxyl radical, are well known for their toxic effects and are produced from normal cellular oxygen metabolism, chemotherapeutic agents, and radiotherapy. The toxic effects generally result in induction of apoptosis and/or necrosis. However, recent studies have shown that ROS are also involved in regulation of gene expression by controlling signal transduction through direct participation in cell signaling (23) and/or modulation of cell redox state (24). The latter results in changes of intracellular GSH and thiol groups in proteins, thus altering the activation of cell signaling proteins. A variety of cell signaling proteins, transcription factors, and cell cycle regulatory proteins are known to be redox sensitive, *e.g.*, p53 (25), p21^{Waf1/Cip1} (26), AP-1 (27), NF- κ B (28), and hypoxia-inducible factor 1 α (29). It is not known if these proteins can be modified by selenium in prostate cancer cells.

In the present study, we investigated the acute and long-term effects of sodium selenite on the LNCaP human prostate cancer cell line and explored possible redox effects of selenium, trying to determine whether cellular redox has a role in anticancer effects of selenium. We hypothesized that selenium functions as a redox modulator to regulate gene expression and modulate apoptosis, resulting in altered cancer cell growth. Our results demonstrated that intracellular redox state was altered by selenite, but the results were different when cells were exposed to selenium acutely *versus* chronically. Our results show that acute treatment of LNCaP cells with selenium results in apoptosis, whereas chronic treatment of the same cells with selenium results in

cell cycle arrest. Both effects suggest the possibility that selenium may inhibit prostate cancer cell growth *in vivo*.

MATERIALS AND METHODS

Chemicals and Antibodies. Sodium selenite, BSO, NAC, and anti- β -actin and anti-Trx antibodies were purchased from Sigma Chemical Co. (St. Louis, MO). MnTMPyP was purchased from Alexis Biochemicals (San Diego, CA). Antimanganese SOD and anticopper, zinc SOD antibodies were a gift from Dr. Larry Oberley (University of Iowa, Iowa City, IA). Anti-Trx Rs 1 and 2 and anti-Trx Pxs I, II, and III antibodies (30, 31) were a gift from Dr. Sue Goo Rhee (NIH, Bethesda, MD). Anti-p27 (C-19) and p21 (C-19) antibodies were purchased from Santa Cruz Biotechnology, Inc. (Santa Cruz, CA). Anti-CAT antibody was purchased from Athens Research & Technology (Athens, GA).

Cell Culture. LNCaP cells were obtained from the American Type Culture Collection and routinely maintained in 100-mm tissue culture dishes (Corning) in RPMI 1640, supplemented with 5% heat-inactivated fetal bovine serum and 1% antibiotic-antimycotic (Life Technologies, Inc., Rockville, MD) at 37°C in a humidified atmosphere of 95% air and 5% CO₂. For selenite adaptation, cells were first grown in media with sodium selenite at 0.5 μ M, and then the doses were increased in a stepwise fashion to allow cells to adapt to higher concentrations of selenite. The adaptation process took 6 months. For biochemical analyses, cells were collected by rinsing in PBS three times, scraping with a rubber policeman in 10-ml PBS, and then centrifuging at 2000 rpm for 5 min. After removing the PBS, the cell pellets were stored at -40°C until use.

Western Blot Analysis. Cell pellets were lysed with M-PER mammalian protein extraction reagent (Pierce, Rockford, IL), and protein concentrations were determined by the Bradford method (Bio-Rad). Cell lysates were electrophoresed in 12% SDS polyacrylamide gels and then transferred onto nitrocellulose membranes. After blotting in 5% nonfat dry milk in 10 mM Tris buffer (pH 7.8) with 0.1% TTBS, the membranes were incubated with primary antibodies at 1:500–1,000 dilutions in TTBS overnight at 4°C, and then secondary antibodies conjugated with horseradish peroxidase added at 1:10,000 dilution in TTBS for 1 h at room temperature. Protein bands were visualized on X-ray film using the enhanced chemiluminescence system (Pierce).

Ultrastructural Analysis of Mitochondria. Confluent cultured cells were washed with PBS, detached by pipeting repeatedly, and fixed in 2.5% glutaraldehyde. Cells were processed for transmission electron microscopy as described previously (32). Cytoplasmic areas were measured from scanned images of the electron micrographs using Scion image software (Scion Corp., Frederick, MD), and mitochondrial numbers were manually counted from the electron micrographs.

GSH Levels. Cells were collected by trypsinization and washed with PBS after selenite treatment. The cells were suspended in phosphate buffer [50 mM potassium phosphate buffer (pH 7.8)], and a small aliquot was used for protein quantitation. For GSH assay, protein precipitation was carried out by mixing one volume of cell suspension with one volume of 10% 5-sulfosalicylic acid and centrifuged at 15,000 rpm for 5 min at 4°C. The supernatants were collected, and total GSH was measured in a DU640 spectrophotometer (Beckman) as described previously (33). Oxidized GSH was indirectly estimated by measuring GSH after the supernatants were incubated in 2-vinylpyridine for 90 min at 4°C.

GPX Activity Assay. Cell pellets were lysed in M-PER mammalian protein extraction reagent, and 200 μ g of cell extracts were used to determine GPX activity as described by Lawrence and Burk (34). One unit of GPX activity was defined as the amount of protein required to oxidize 1 μ mol of NADPH per min.

Cell Growth Analysis. Cells were seeded at 2×10^4 cells/well in 12-well plates with or without selenite, and media were changed every 3 days. After trypsinization, cell numbers were counted every 3 days using a hemocytometer.

Cytotoxicity Assay. Cells were seeded at 2×10^4 cells/well in 24-well plates overnight before treatment with different agents and then allowed to grow for an additional 72 h. MTT assay was used to estimate cell viability as described previously (35).

Flow Cytometric Analysis. Cell samples were prepared and analyzed as described previously (36). After selenite treatment and trypsinization, 1×10^6

cells were washed with PBS/EDTA/BSA buffer (PBS, 1 mM EDTA, and 0.1% BSA) and fixed in 100 μ l of PBS/EDTA/BSA buffer + 900 μ l of 70% ethanol for 30 min at -20°C. After washing with phosphate-citric acid buffer [0.192 M Na₂HPO₄ and 4 mM citric acid (pH 7.8)], the cells were stained in 500 μ l of propidium iodide staining solution (33 μ g/ml propidium iodide, 200 μ g/ml DNase-free RNase A, and 0.2% Triton X-100) overnight at 4°C. Both cell cycle distribution and apoptotic cells were simultaneously measured in a FACScan flow cytometer (Becton Dickinson) using 488-nm laser excitation. Intracellular ROS were determined using 2',7'-dichlorofluorescein diacetate as described previously (37).

Statistical Analysis. Tukey's multiple comparison and ANOVA analysis were used to determine the significance of statistical difference of the data at the level of $P < 0.05$ using SYSTAT computer statistics software (SPSS, Inc., Chicago, IL).

RESULTS

Effects of Sodium Selenite on Cytotoxicity and Cell Growth.

Cell viability of LNCaP prostate carcinoma cells was measured using the MTT assay after 72-h treatments with selenite and other agents. A dose-response survival curve of selenite-induced acute cytotoxicity is shown in Fig. 1A. Acute cytotoxicity induced by selenite occurred at 1 μ M concentration, increased as doses increased, and was maximal at 2.5 μ M. Cell viability was 81% of control ($P < 0.001$) at 1 μ M and 8% at 2.5 μ M ($P < 0.0001$). Cell growth was determined by counting cell numbers with a hemocytometer at different concentrations of selenite and at different time points (Fig. 1B). Significant cell growth inhibition ($P < 0.05$) was seen at doses of 1.5 and 2 μ M selenite on day 3 and after but was not seen at 0.5 μ M concentration until day 6. However, cell growth inhibition at 0.5 μ M selenite was much less than that at 1.5 and 2 μ M concentrations.

Fig. 1C shows the effects of selected redox-modulating agents on

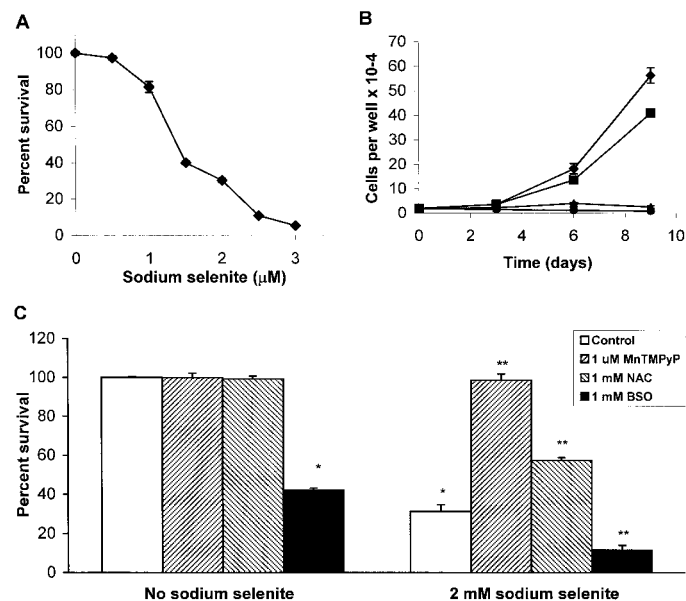


Fig. 1. A, MTT assay of acute cytotoxicity of sodium selenite in LNCaP cells without selenite adaptation. Percentage of survival is cell viability relative to control (0 μ M). Data represent mean \pm SD, $n = 3$. Significant ($P < 0.05$) cell killing occurred at ≥ 1 μ M concentration of selenite. B, effects of selenite on cell growth in LNCaP cells without selenite adaptation; control (\blacklozenge), 0.5 μ M selenite (\blacksquare), 1.5 μ M selenite (\blacktriangle), 2 μ M selenite (\bullet). Cell numbers were counted using a hemocytometer. Data represent mean \pm SD, $n = 3$. Significant ($P < 0.05$) cell killing occurred on day 3 in 1.5 and 2 μ M selenite but not until day 6 in 0.5 μ M selenite. C, modulation of acute cytotoxicity of sodium selenite by antioxidants MnTMPyP and NAC and prooxidant BSO in nonadapted LNCaP cells. Cell viability was determined by MTT assay, and percentage of viability is relative to control without selenite. Data represent mean \pm SD, $n = 3$. *, $P < 0.001$ compared with control cells without selenite; **, $P < 0.001$ compared with control cells treated with 2 μ M selenite alone.

selenite-induced acute cytotoxicity. When 1 μM MnTMPyP, a synthetic SOD mimic, was present, selenite-induced acute cytotoxicity was completely prevented. This was in a dose-dependent manner, reaching maximal protection at 1 μM MnTMPyP for cells treated with 2 μM selenite. The protection was also dependent on the selenite concentrations; higher concentration of selenite required higher concentrations of MnTMPyP (data not shown). Acute cytotoxicity was also significantly decreased when 1 mM NAC was present, but NAC protection was not as effective as MnTMPyP, and there was no additional protection when concentrations of NAC were increased (data not shown). In contrast, treatment with 1 mM BSO, a γ -glutamyl cysteine synthetase inhibitor, resulted in cell growth inhibition and significantly enhanced selenite-induced acute cytotoxicity in a dose-dependent fashion. Flow cytometric analysis showed that the acute cytotoxicity induced by selenite was mediated by a dose-dependent induction of apoptosis (Fig. 2), and cells showed a 2-fold increase in

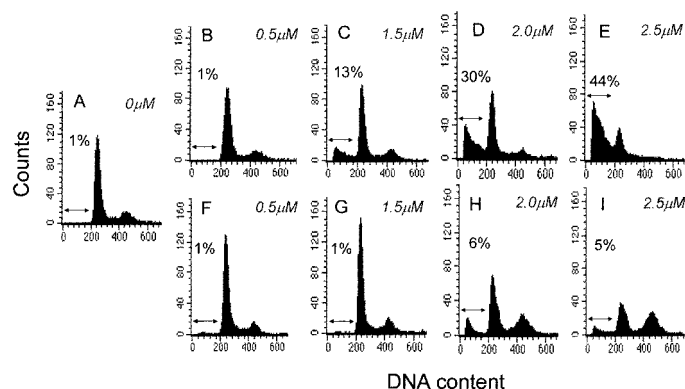


Fig. 2. Histograms of flow cytometric analysis showing effects of selenite on apoptosis and cell cycle in LNCaP cells; control cells (A), nonadapted cells treated with 0.5–2.5 μM selenite for 24 h (B–E), and selenite-adapted cells treated with 0.5–2.5 μM selenite (F–I). The percentage of apoptotic cells is indicated above each hypodiploid (sub-G₁) peak. The data represent one of two independent experiments.

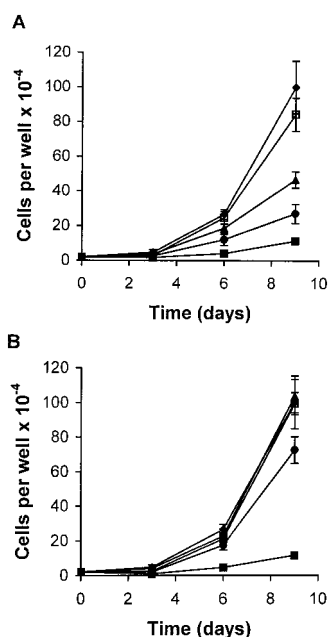


Fig. 3. Effects of sodium selenite on cell growth in LNCaP cells adapted to different concentrations of selenite. A, adapted cells continuously treated with selenite; B, adapted cells in which selenite was removed at time 0 to test reversibility of adaptive growth changes. Control (◆), 0.5 μM selenite (▲), 1.5 μM selenite (●), 2.0 μM selenite (●), and 2.5 μM selenite (■). Cell numbers were determined using a hemocytometer. Data represent mean \pm SD, $n = 3$.

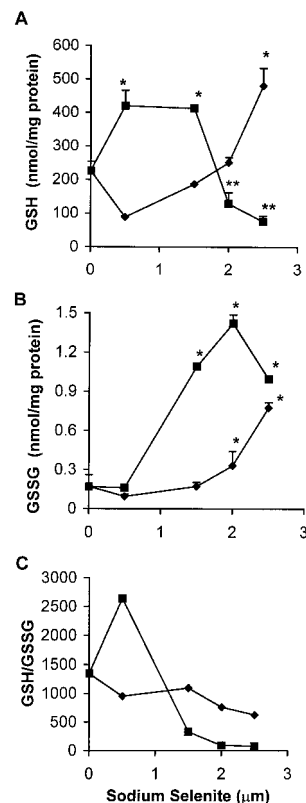


Fig. 4. Effects of selenite on intracellular levels of GSH, GSSG, and the ratio of GSH:GSSG in LNCaP cells with and without selenite adaptation. ■, nonadapted cells; ◆, selenite-adapted cells. Data represent mean \pm SD, $n = 3$. *, significant increase compared with control, $P < 0.001$; **, significant decrease compared with control, $P < 0.001$.

dichlorofluorescein fluorescence in 15 min after treatment with 2.5 μM selenite (data not shown).

Because possible clinical cancer chemoprevention and cancer therapy by selenium are long-term interventions, we developed selenite-adapted cells from the LNCaP cell line by exposing cells to a stepwise increase in selenite concentrations over 6 months. LNCaP cells gradually adapted to toxic levels of selenite and grew continuously at much higher concentrations of selenite. This allowed us to evaluate the long-term effects of selenium on cancer cells *in vitro*. Although LNCaP cells adapted to toxic concentrations of sodium selenite since continuous cell growth occurred, adaptation was not complete because cell growth rates were much slower at ≥ 1.5 μM doses of selenite than the untreated control (Fig. 3A). There was no difference in growth rate between 0.5 μM selenite and the control. The selenite-adapted cells had much lower apoptosis than the nonadapted cells when exposed to sodium selenite, and apoptosis after selenite exposure in these adapted cells was only slightly higher than the control (Fig. 2). To test reversibility of selenite adaptation, selenite was removed from the media; cell growth inhibition in the adapted cells was reversible at ≤ 2.0 μM concentrations of selenite but not reversible at 2.5 μM concentration for at least ≤ 9 days after removal of selenite (Fig. 3B).

Effects of Selenium on Intracellular GSH and GSSG. Because oxidative stress was induced by treatment with selenite, we decided to determine intracellular redox state by measuring cellular GSH and GSSG. After LNCaP cells were treated with selenite for 24 h, the intracellular levels of GSH were increased at doses of 0.5 and 1.5 μM selenite and decreased at doses of 2 and 2.5 μM selenite (Fig. 4A). However, the levels of GSSG were increased from 1.5 to 2.5 μM selenite (Fig. 4B). The ratio of GSH:GSSG was biphasic with increased ratio at 0.5 μM selenite and decreased ratio at higher doses

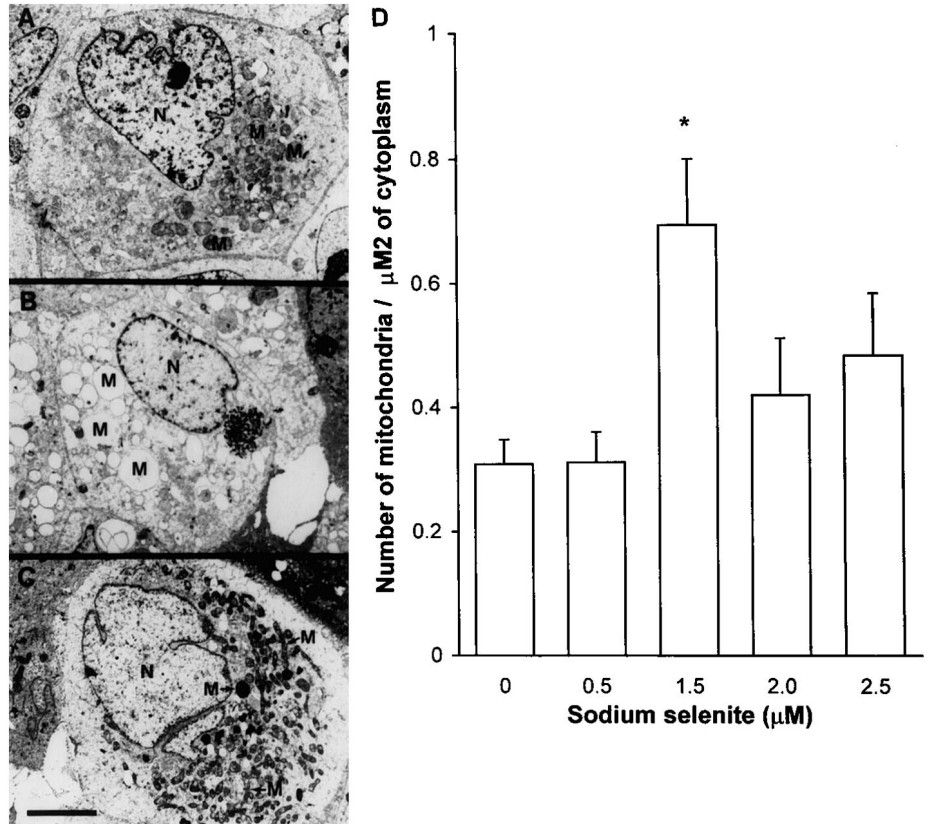


Fig. 5. Transmission electron microscopy showing effects of selenite on number and morphology of mitochondria in LNCaP cells with and without selenite adaptation. *A*, control; *B*, nonadapted cells treated with 2.5 μM selenite for 24 h; *C*, selenite-adapted cells with 2.5 μM selenite. *M*, mitochondrion; *N*, nucleus. Mitochondria in nonadapted cells showed swelling and loss of cristae, whereas mitochondria in selenite-adapted cells were increased in size and number compared with control. The internal scale represents 5 μm. *D*, effects of selenite on number of mitochondria in LNCaP cells with selenite adaptation. Data represent mean ± SE, $n = 14-27$. *, $P = 0.005$ compared with control (0 μM selenite).

(Fig. 4C). In contrast, the selenite-adapted cells demonstrated a decrease in the levels of GSH at doses of 0.5 and 1.5 μM selenite and an increase in the levels of GSH at doses 2 and 2.5 μM selenite (Fig. 4A). The levels of GSSG showed a similar pattern to the nonadapted cells with increased GSSG as dose increased, though GSSG increased at 1.5 μM selenite in the nonadapted cells but did not increase until 2 μM in the adapted cells (Fig. 4B). The ratio of GSH:GSSG was only slightly decreased in a dose-dependent manner in the selenite-adapted cells (Fig. 4C), and the magnitudes of decrease were much lower than those of the nonadapted cells.

Effects of Selenite on Mitochondria. Transmission electron microscopy showed that selenite-induced acute cytotoxicity resulted in mitochondrial injury, as demonstrated by mitochondrial swelling and loss of cristae (Fig. 5B). Mild mitochondrial injury was present at 0.5 μM selenite, and the injury increased as selenite concentration increased. It was difficult to differentiate severely injured mitochondria from other cellular organelles, such as endoplasmic reticulum, because vacuolization was also seen in other organelles. Typical apoptotic cells with chromosome condensation and nuclear fragmentation were observed in cells treated with 1.5–2.5 μM selenite (data not shown), which correlated with the flow cytometric data. In the selenite-adapted cells, the mitochondria showed only mild damage, with most mitochondria appearing normal; however, a few (<10%) mitochondria had a higher electron density and very minor focal loss of cristae (Fig. 5C). The mitochondria from selenite-adapted cells showed a significant increase in number (Fig. 5D) and elongation in shape (Fig. 5C) at ≥1.5 μM selenite.

Effects of Selenite on GPX Activity, Antioxidant Enzymes, and Cyclin-dependent Kinase Inhibitors. Enzymatic analysis showed that GPX activities in the selenite-adapted cells were significantly increased (2- to 3-fold induction; Fig. 6A). Enzymatic activity induction was similar between 0.5 and 2 μM selenite, but GPX activity at 2.5 μM was slightly higher than those at lower doses ($P < 0.001$

compared with ≤2.0 μM). When 1.5 and 2.5 μM selenite-adapted cells were switched to media without selenite for 2 weeks, GPX activities were significantly decreased in both selenite-adapted cell cultures, but activities were still significantly higher than that in the control cells (Fig. 6B). The rates of decrease in GPX activity after selenite removal were similar between 1.5 and 2.5 μM selenite-adapted cells (data not shown).

Western blotting showed that MnSOD immunoreactive protein was induced at ≥1.5 μM concentrations of selenite (Fig. 7). CuZnSOD immunoreactive protein levels were increased at ≥1.5 μM concentrations of selenite. There were no changes in CAT immunoreactive protein levels. In the Trx and Trx R system, immunoreactive protein of Trx R2 was induced and reached a peak value at 0.5 μM selenite. Trx Px II immunoreactive protein levels were also induced but not until a level of 2.5 μM selenite (Fig. 7). There were no changes in Trx, Trx R1, Trx Px I, and Trx Px III immunoreactive protein levels (Fig. 7) after exposure to sodium selenite. Cyclin-dependent kinase inhibitors p21^{Waf1/Cip1} and p27^{Kip1} immunoreactive protein levels were induced (Fig. 7). p21^{Waf1/Cip1} was induced only at ≥1.5 μM doses of selenite. p27^{Kip1} was induced at 0.5 μM selenite, but there was no additional induction at higher doses. β-actin, used as a control for protein loading, showed no difference among all of the selenite doses studied.

Similar to the results of GPX, the levels of MnSOD and p21^{Waf1/Cip1} immunoreactive proteins were decreased in both 1.5 and 2.5 μM selenite-adapted cells after selenite removal for 2 weeks, compared with levels in selenite-adapted cells in which selenite continued to be present in the media. The level of p21^{Waf1/Cip1} was even lower in the 1.5 μM than in the control cells (Fig. 8). In contrast, the levels of CuZnSOD immunoreactive protein in 1.5 and 2.5 μM selenite-adapted cells showed no change after selenite removal and were higher than that in the control cells (Fig. 8). Levels of CAT, p27^{Kip1},

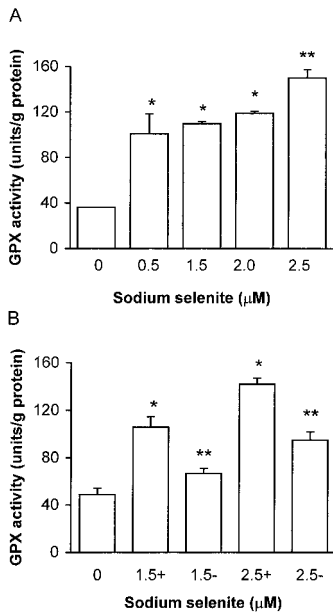


Fig. 6. Effects of selenite on GPX activity in LNCaP cells with selenite adaptation. A, cells were grown in media with selenite corresponding to their adapted doses. Data represent mean ± SD, n = 3. *, P < 0.001 compared with control; **, P < 0.001 compared with control and 0.5 μM. B, effects of selenite on GPX activity in selenite-adapted LNCaP cells before and after selenite removal. 0, control; 1.5+, 1.5 μM selenite-adapted cells with 1.5 μM selenite; 1.5-, 1.5 μM selenite-adapted cells but without selenite for 2 weeks; 2.5+, 2.5 μM selenite-adapted cells with 2.5 μM selenite; 2.5-, 2.5 μM selenite-adapted cells but without selenite for 2 weeks. Data represent mean ± SD, n = 3. *, P < 0.001 compared with control (0 μM selenite); **, P < 0.05 compared with control and P < 0.001 compared with corresponding adapted cells without selenite removal.

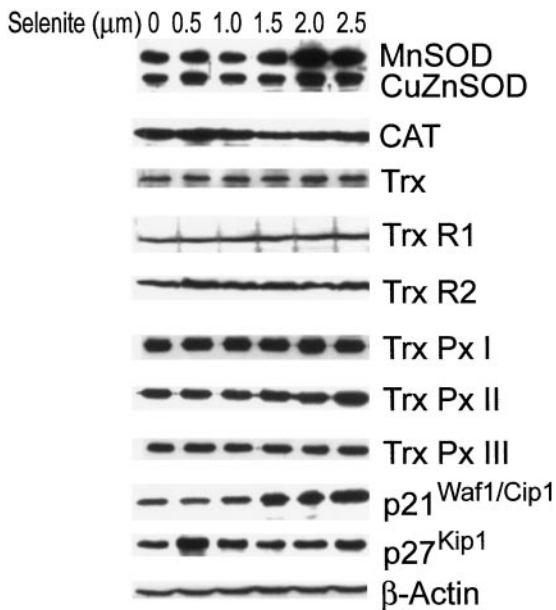


Fig. 7. Western blot analysis of selected immunoreactive proteins in selenite-adapted LNCaP cells. Levels of selenite adaptation are indicated above each lane. Protein loading: MnSOD, CuZnSOD, CAT, and β-actin, 15 μg; Trx and Trx Px I, II, and III, 20 μg; Trx R I and II, p21^{Waf1/Cip1}, and p27^{Kip1}, 40 μg.

and β-actin were not regulated by changing the status of selenite in the culture media (Fig. 8).

Effects of Selenite on Cell Cycle Distribution. Flow cytometric analysis showed no changes in cell cycle distribution at 24 h in the nonadapted cells treated acutely with selenite at low concentrations; it was not possible to calculate cell cycle distribution at high concen-

trations because of interference in histogram analysis by large numbers of apoptotic cells (data not shown). Selenite-adapted cells were arrested in G₂-M phase of the cell cycle and also showed a decrease in S phase at doses of 1.5–2.5 μM selenite in a dose-dependent manner (Table 1). The percentage of cells in G₀-G₁ phase was decreased at 2 and 2.5 μM concentrations of selenite.

DISCUSSION

Recent studies have suggested that selenium may be a potential chemopreventive agent for prostate cancer (11, 14). However, the underlying mechanisms of cancer chemoprevention by selenium remain to be elucidated. Additionally, acute treatment of prostate cancer cells *in vitro* has been shown to result in apoptosis (17, 18). To date, most experimental studies have investigated only the acute effects of selenium on cell growth inhibition and cytotoxicity. Although there are several studies of human prostate cancer cells (6, 16–18), at least one of them studied the molecular mechanisms of selenium action in prostate cancer chemoprevention and cancer therapy. In the clinical setting, prostate cancer chemoprevention and cancer therapy are long-term interventions, in which only nontoxic doses of selenium are used (38). In the present study, we studied the LNCaP prostate cancer cell line, an androgen-sensitive cell line, to investigate possible redox-regulated mechanisms of selenium in acute anticancer effects. We also developed selenium-adapted cells from the LNCaP cell line, which allowed us to evaluate the long-term effects of selenium in human prostate cells. Our results demonstrated that anticancer effects of selenium were mediated via a redox mechanism involving induction of oxidative stress, as determined by alterations in intracellular GSH levels in LNCaP human prostate cancer cells. However, the *in vitro* biological consequences of selenite exposure were different between acute and long-term exposure. In acute exposure, selenite caused cell death, mainly apoptosis attributable to oxidative stress; in chronic long-term exposure, selenite caused only minimal cell death but inhibited cell growth by modifying gene expression and cell cycle progression.

Both acute and chronic exposure to selenite resulted in altered GSH

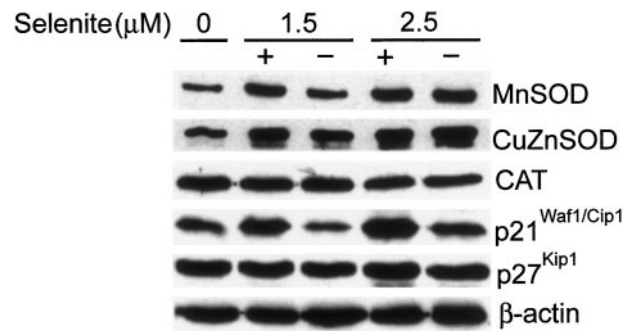


Fig. 8. Western blot analysis of levels of MnSOD, CuZnSOD, CAT, p21^{Waf1/Cip1}, p27^{Kip1}, and β-actin immunoreactive proteins in 1.5 and 2.5 μM selenite-adapted LNCaP cells before and after selenite removal. Levels of original selenite adaptation and presence (+) or absence (-) of subsequent selenite to test for reversibility are indicated above each lane. Selenite was removed from culture media for 2 weeks. Protein loading: MnSOD, CuZnSOD, CAT, and β-actin, 10 μg; p21^{Waf1/Cip1} and p27^{Kip1}, 30 μg.

Table 1 Effects of selenite on cell cycle distribution in selenite-adapted LNCaP cells

Selenite (μM)	G ₀ G ₁ (%)	S (%)	G ₂ M (%)
0	70.88	18.25	10.84
0.5	69.68	21.56	8.55
1.5	71.44	16.24	12.33
2.0	52.01	14.85	33.14
2.5	38.85	11.14	50.01

and GSSG levels. However, the selenite-adapted cells were able to maintain a more optimal cellular GSH:GSSG ratio after exposure to selenite, and this may partially explain the resistance of these cells to selenite exposure. The mechanism(s) by which GSH and GSSG are altered in selenite-adapted cells is not known, but induction of GPX could use GSH and simultaneously increase GSSG levels. Intracellular GSH is a key redox regulator that is crucial for multiple biological functions. The GSH:GSSG ratio usually is an important measure of intracellular redox balance. Increased GSSG indicates a shift in the redox equilibrium toward oxidation. This change will alter protein cysteinyl residues and, in turn, may alter protein-protein and protein-DNA interactions and result in modulation of redox-sensitive enzymes, cell signaling proteins, and cell cycle-regulatory proteins. Therefore, altered gene expression, resulting in altered regulation of cell growth and/or cell death, may occur, depending on the levels and location of redox shift. In our study, the redox shift by selenite was probably beyond the limit of cell tolerance in the nonadapted cells treated with selenite, and, therefore, the cells underwent apoptosis. In contrast, GSSG increased to a high level in the selenite-adapted cells only at the highest concentration tested (2.5 μM), and therefore, the cells could survive more readily than the nonadapted cells. Oxidative stress may also explain why selenite-adapted cells had alteration of expression of selected genes.

Mitochondria are vital organelles in eukaryotic cells. These organelles are well known to function in cellular energy metabolism, resulting in the production of cellular ATP. In addition, mitochondria are known to be a major source of intracellular ROS, resulting from aerobic metabolism. Recent studies have demonstrated that mitochondria also play a central role in controlling cell apoptosis (39). In our study, mitochondria exhibited severe injury in selenite-induced acute cytotoxicity, as demonstrated by loss of cristae and vacuolization. These changes occurred before typical apoptotic changes (data not shown). Flow cytometric analysis demonstrated an increase in hypodiploid cells, indicative of cells undergoing apoptosis. In contrast, selenite-adapted cells showed a significant increase in size and number of mitochondria, and these mitochondria showed much less damage. Flow cytometric analysis showed only minimal increase in hypodiploid cells in selenite-adapted cells, indicating much fewer apoptotic cells compared with nonadapted cells. Our results suggest that mitochondria are probably the primary target of cell killing by selenite. MnSOD and Trx R2 are both mitochondrial enzymes, and both show a large increase in immunoreactive protein levels in selenite-adapted cells after treatment with selenite. In addition, GPX is known to be localized in every compartment of the cell, including mitochondria (40). An increase in mitochondria may be one mechanism of cell adaptation to selenite after chronic long-term treatment. The biological significance of this adaptation is not clear. It may result in cancer cell resistance to selenium or may alter cell redox state modulating cancer cell growth. Increased number and size of mitochondria are also seen during epithelial cell differentiation. Future studies are needed to clarify the role of mitochondria in selenite-induced toxicity after adaptation.

Selenium has been well known as a nutritional requirement in maintaining human and animal health. The most important function of selenium in human health is its antioxidant activity resulting from its presence in the enzymatic active site of GPX (1) and Trx Rs (2). This antioxidant function of selenium is also considered to be the probable mechanism of cancer prevention. Evidence supporting this hypothesis was provided from epidemiological studies, which demonstrated that people with low levels of plasma selenium had high incidence of cancer (8–10). However, animal studies (19) and clinical trials in humans (11) showed that the dosages of selenium required for cancer prevention were at least 10 times higher than that of dietary require-

ments necessary to reach optimal antioxidant activity. In the present study, we demonstrated that GPX activity and Trx R immunoreactive proteins reached maximum levels at 0.5 μM selenite, a level which did not result in significant cell growth inhibition. These results demonstrate that GPX activity and immunoreactive protein levels of Trx Rs did not strictly correlate with cancer cell growth inhibition and suggest the possibility that the antioxidant functions of selenite do not correlate with cancer cell growth inhibition. Our study does not address the potential effects of selenium antioxidant activity on tumor initiation and promotion because the model system used in our study is a cancer cell line that has already presumably undergone the early stages of cancer development. Protection of DNA damage from oxidation by GPX has been considered to be the potential mechanism by which selenium prevents tumor initiation (4).

In addition to its antioxidant activity, selenium is known to be toxic at high levels, which is proposed to be one of the possible anticancer mechanisms. When selenite undergoes redox metabolism, GSH is consumed, whereas GSSG and ROS, especially superoxide, are produced (7, 19, 22). This can shift the cellular redox balance to a relative oxidative state. This change may result in two possible consequences to cells, depending on the dose, duration, and intracellular detoxifying systems: (a) it may cause cell death when the production of ROS, oxidation of GSH, and resultant production of GSSG are beyond the limit of cell tolerance; and (b) it may modify biological functions of the cells when the changes are still within the limits of cell tolerance. Superoxide may be the main ROS produced by selenite because an SOD mimic was the most effective agent demonstrated to prevent selenite cytotoxicity. These results and conclusions are in agreement with previous studies by other laboratories (7, 22). A decrease in GSH and an increase in GSSG could be explained by both selenite redox metabolism and oxidative stress at high concentrations of selenite. Sublethal damage may occur in selenite-adapted cells in which the cells continuously grew in toxic levels of selenite.

MnSOD has been shown to be generally low in most types of cancers compared with their normal counterparts (41). Suppression of the malignant phenotype by overexpression of MnSOD has been demonstrated in a variety of tumor cell lines (42–46). Up-regulation of MnSOD in selenite-adapted LNCaP cells may be attributable to oxidative stress caused by production of superoxide generated from selenite redox metabolism. Increased MnSOD may protect cells from oxidative damage and may also inhibit cancer cell growth. In addition, an increase in MnSOD may change intracellular redox state by converting superoxide into hydrogen peroxide, which, in turn, modifies expression of redox-sensitive genes (47). Modification of NF- κ B and AP-1 activities was demonstrated in MnSOD-overexpressing MCF-7 human breast cancer cells (48). We have shown up-regulation of p21^{Waf1/Cip1} after overexpression of MnSOD in a *ras*-transformed human prostate epithelial cell line.⁴ Conversely, it has been demonstrated that overexpression of p21^{Waf1/Cip1} up-regulated MnSOD expression (49). The exact relationship between MnSOD and p21^{Waf1/Cip1} is not clear, but both genes have been shown to function in regulation of cancer cell growth. Evidence from these studies supports the potential influence of MnSOD on intracellular redox state that may, in turn, alter transcription factor activity, gene expression, and cell growth and differentiation. It is also possible that both MnSOD and p21^{Waf1/Cip1} are independently up-regulated by selenite via an oxidative mechanism.

Cell cycle arrest at G₂-M phase by selenium has been shown in studies by others (50). Several studies have shown that overexpression of p21^{Waf1/Cip1} resulted in a cell cycle arrest at G₂-M phase (51–53).

⁴ Unpublished observations.

Previous studies have also demonstrated that genistein-induced cell cycle arrest at G₂-M phase and cell growth inhibition in human breast and prostate cancer cells were associated with the induction of p21^{Waf1/Cip1} (54–56). A G₂-M cell cycle arrest by oxidative stress is thought to be primarily attributable to DNA damage, which delays cell cycle progression, thus allowing repair of damaged DNA. G₂-M cell cycle arrest induced by selenite may be caused by oxidative stress and/or up-regulation of p21^{Waf1/Cip1}. This may be the reason why the selenite-adapted cells grew much slowly, although they continued to grow in toxic levels of selenite.

It is unclear whether selenite adaptation would result in resistance of cancer cells to selenium anticancer effects. Our results showed that cell growth inhibition remained when selenite was present in the culture medium. However, cell growth inhibition was reversible when selenite was removed from the culture medium. The reversibility was dose and time dependent. Cells grown in higher dose selenite recovered more slowly than cells grown in low dose selenite; cells grown in 2.5 μM selenite showed no significant reversal of cell growth inhibition (Fig. 3B) ≤9 days after selenite removal but showed significant reversal at 2 weeks (data not shown). When cells were re-exposed to corresponding concentrations of selenite after 2 weeks of selenite removal, they still maintained resistance to selenite and showed growth inhibition (data not shown). Our results suggest that there may be different biochemical mechanisms controlling selenite adaptation and selenite-induced cell growth inhibition. Our results show that elevated CuZnSOD expression more closely correlated with selenite adaptation, whereas elevated MnSOD and p21^{Waf1/Cip1} more closely correlated to cell growth inhibition.

In summary, our results demonstrate that intracellular redox state as measured by cellular GSH and GSSG levels was altered by sodium selenite. However, the consequences were different after acute *versus* chronic treatment. In acute treatment, selenite caused mitochondrial damage and induced apoptosis in LNCaP cells. In chronic treatment, LNCaP cells adapted to selenite cytotoxicity by altering their antioxidant defense systems and modifying intracellular redox state. Apoptosis was dramatically decreased in selenite-adapted cells. Selenite-adapted cells also showed a slow growth rate and up-regulation of multiple proteins, some of which are redox sensitive and have cell growth inhibition functions. Some of these up-regulated proteins are known to be located in the mitochondria. Our results suggest that redox-regulated anticancer effects may be one of the mechanisms of cancer chemoprevention by selenium. Our results also suggest that alteration of intracellular redox state by modifying cellular antioxidants and antioxidant enzymes may regulate therapeutic effectiveness of selenium in prostate cancer therapy.

ACKNOWLEDGMENTS

We thank Jamie McMaster, Joan Sempf, and Kathy Schell for technical assistance. We also thank Drs. Larry Oberley and Sue Goo Rhee for critical reading of this manuscript.

REFERENCES

- Rotruck, J. T., Pope, A. L., Ganther, H. E., Swanson, A. B., Hafeman, D. G., and Hoekstra, W. G. Selenium: biochemical role as a component of glutathione peroxidase. *Science (Wash. DC)*, *179*: 588–590, 1973.
- Powis, G., Gasdaska, J. R., Gasdaska, P. Y., Berggren, M., Kirkpatrick, D. L., Engman, L., Cotgreave, I. A., Angulo, M., and Baker, A. Selenium and the thioredoxin redox system: effects on cell growth and death. *Oncol. Res.*, *9*: 303–312, 1997.
- Gallegos, A., Berggren, M., Gasdaska, J. R., and Powis, G. Mechanisms of the regulation of thioredoxin reductase activity in cancer cells by the chemopreventive agent selenium. *Cancer Res.*, *57*: 4965–4970, 1997.
- Ip, C. Prophylaxis of mammary neoplasia by selenium supplementation in the initiation and promotion phases of chemical carcinogenesis. *Cancer Res.*, *41*: 4386–4390, 1981.
- Redman, C., Xu, M. J., Peng, Y.-M., Scott, J. A., Payne, C., Clark, L. C., and Nelson, M. A. Involvement of polyamines in selenomethionine induced apoptosis and mitotic alterations in human tumor cells. *Carcinogenesis (Lond.)*, *18*: 1195–1202, 1997.
- Redman, C., Scott, J. A., Baines, A. T., Basye, J. L., Clark, L. C., Calley, C., Roe, D., Payne, C. M., and Nelson, M. A. Inhibitory effect of selenomethionine on the growth of three selected human tumor cell lines. *Cancer Lett.*, *125*: 103–110, 1998.
- Shen, H.-M., Yang, C.-F., and Ong, C.-N. Sodium selenite-induced oxidative stress and apoptosis in human hepatoma HepG₂ cells. *Int. J. Cancer*, *81*: 820–828, 1999.
- Shamberger, R. J., Tytko, S. A., and Willis, C. E. Antioxidants and cancer. Part VI. Selenium and age-adjusted human cancer mortality. *Arch. Environ. Health*, *31*: 231–235, 1976.
- Schrauzer, G. N., White, D. A., and Schneider, C. J. Cancer mortality correlation studies. III. Statistical association with dietary selenium intakes. *Bioinorg. Chem.*, *7*: 35–56, 1977.
- Clark, L. C., Cantor, K. P., and Allaway, W. H. Selenium in forage crops and cancer mortality in US counties. *Arch. Environ. Health*, *46*: 37–42, 1991.
- Clark, L. C., Combs, G. F., Jr., Turnbull, B. W., Slate, E. H., Chalker, D. K., Chow, J., Davis, L. S., Glover, R. A., Graham, G. F., Gross, E. G., Krongrad, A., Leshner, J. L., Jr., Park, H. K., Sanders, B. B., Jr., Smith, C. L., and Taylor, J. R. Effects of selenium supplementation for cancer prevention in patients with carcinoma of the skin. A randomized controlled trial. Nutritional Prevention of Cancer Study Group. *JAMA*, *276*: 1957–1963, 1996.
- Yu, S. Y., Zhu, Y. J., Li, W. G., Huang, Q. S., Huang, C. Z., Zhang, Q. N., and Hou, C. A preliminary report on the intervention trials of primary liver cancer in high-risk populations with nutritional supplementation of selenium in China. *Biol. Trace Elem. Res.*, *29*: 289–294, 1991.
- Blot, W. J., Li, J. Y., Taylor, P. R., Guo, W., Dawsey, S., Wang, G. Q., Yang, C. S., Zheng, S. F., Gail, M., Li, G. Y., Yu, Y., Liu, B. Q., Tangrea, J., Sun, Y. H., Liu, F., Fraumeni, J. F., Zhang, Y. H., and Li, B. Nutrition intervention trials in Linxian, China: supplementation with specific vitamin/mineral combinations, cancer incidence, and disease-specific mortality in the general population. *J. Natl. Cancer Inst. (Bethesda)*, *85*: 1483–1492, 1993.
- Yoshizawa, K., Willett, W. C., Morris, S. J., Stampfer, M. J., Spiegelman, D., Rimm, E. B., and Giovannucci, E. Study of prediagnostic selenium level in toenails and the risk of advanced prostate cancer. *J. Natl. Cancer Inst. (Bethesda)*, *90*: 1219–1224, 1998.
- Greenlee, R. T., Murray, T., Bolden, S., and Wingo, P. A. Cancer statistics, 2000. *CA Cancer J. Clin.*, *50*: 7–33, 2000.
- Webber, M. M., Perez-Ripoll, E. A., and James, G. T. Inhibitory effects of selenium on the growth of DU-145 human prostate carcinoma cells *in vitro*. *Biochem. Biophys. Res. Commun.*, *130*: 603–609, 1985.
- Vadgama, J. V., Wu, Y., Shen, D., and Block, J. Effects of selenium in combination with adriamycin or taxol on several different cancer cells. *Anticancer Res.*, *20*: 1391–1414, 2000.
- Menter, D. G., Sabichi, A. L., and Lippman, S. M. Selenium effects on prostate cell growth. *Cancer Epidemiol. Biomarkers Prev.*, *9*: 1171–1182, 2000.
- Combs, G. F., Jr., and Gray, W. P. Chemopreventive agents: selenium. *Pharmacol. Ther.*, *79*: 179–192, 1998.
- Ganther, H. E. Selenium metabolism, selenoproteins and mechanisms of cancer prevention: complexities with thioredoxin reductase. *Carcinogenesis (Lond.)*, *20*: 1657–1666, 1999.
- Jiang, C., Jiang, W., Ip, C., Ganther, H., and Lu, J. Selenium-induced inhibition of angiogenesis in mammary cancer at chemopreventive levels of intake. *Mol. Carcinog.*, *26*: 213–225, 1999.
- Kitahara, J., Seko, Y., and Imura, N. Possible involvement of active oxygen species in selenite toxicity in isolated rat hepatocytes. *Arch. Toxicol.*, *67*: 497–501, 1993.
- Finkel, T. Oxygen radicals and signaling. *Curr. Opin. Cell Biol.*, *10*: 248–253, 1998.
- Dalton, T. P., Shertzer, H. G., and Puge, A. Regulation of gene expression by reactive oxygen. *Annu. Rev. Pharmacol. Toxicol.*, *39*: 67–101, 1999.
- Hainaut, P., and Milner, J. Redox modulation of p53 conformation and sequence-specific DNA binding *in vitro*. *Cancer Res.*, *53*: 4469–4473, 1993.
- Qiu, X., Forman, H. J., Schonthal, A. H., and Cadenas, E. Induction of p21 mediated by reactive oxygen species formed during the metabolism of aziridinylbenzoquinones by HCT116 cells. *J. Biol. Chem.*, *271*: 31915–31921, 1996.
- Abate, C., Patel, L., Rauscher, F. J., III, and Curran, T. Redox regulation of fos and jun DNA-binding activity *in vitro*. *Science (Wash. DC)*, *249*: 1157–1161, 1990.
- Toledano, M. B., and Leonard, W. J. Modulation of transcription factor NF-κB binding activity by oxidation-reduction *in vitro*. *Proc. Natl. Acad. Sci. USA*, *88*: 4328–4332, 1991.
- Wang, G. L., and Semenza, G. L. Characterization of hypoxia-inducible factor 1 and regulation of DNA binding activity by hypoxia. *J. Biol. Chem.*, *268*: 21513–21518, 1993.
- Lee, S. R., Bar-Noy, S., Kwon, J., Levine, R. L., Stadtman, T. C., and Rhee, S. G. Mammalian thioredoxin reductase: oxidation of the C-terminal cysteine/selenocysteine active site forms a thioselenide, and replacement of selenium with sulfur markedly reduces catalytic activity. *Proc. Natl. Acad. Sci. USA*, *97*: 2521–2526, 2000.
- Kang, S. W., Chae, H. Z., Seo, M. S., Kim, K., Baines, I. C., and Rhee, S. G. Mammalian peroxiredoxin isoforms can reduce hydrogen peroxide generated in response to growth factors and tumor necrosis factor-α. *J. Biol. Chem.*, *273*: 6297–6302, 1998.
- Yang, A. H., Gould-Kostka, J., and Oberley, T. D. *In vitro* growth and differentiation of human kidney tubular cells on a basement membrane substrate. *In Vitro Cell. Dev. Biol.*, *23*: 34–46, 1987.

33. Li, N., Oberley, T. D., Oberley, L. W., and Zhong, W. Inhibition of cell growth in NIH/3T3 fibroblasts by overexpression of manganese superoxide dismutase: mechanistic studies. *J. Cell. Physiol.*, *175*: 359–369, 1998.
34. Lawrence, R. A., and Burk, R. F. Glutathione peroxidase activity in selenium-deficient rat liver. *Biochem. Biophys. Res. Commun.*, *71*: 952–958, 1976.
35. Zhong, W., Oberley, L. W., Oberley, T. D., Yan, T., Domann, F. E., and St. Clair, D. K. Inhibition of cell growth and sensitization to oxidative damage by overexpression of manganese superoxide dismutase in rat glioma cells. *Cell Growth Differ.*, *7*: 1175–1186, 1996.
36. Darzynkiewicz, Z., Li, X., and Gong, J. Assays of cell viability: discrimination of cells dying by apoptosis. *Methods Cell Biol.*, *41*: 15–38, 1994.
37. Li, N., and Oberley, T. D. Modulation of antioxidant enzymes, reactive oxygen species, and glutathione levels in manganese superoxide dismutase-overexpressing NIH/3T3 fibroblasts during the cell cycle. *J. Cell. Physiol.*, *177*: 148–160, 1998.
38. Nelson, M. A., Porterfield, B. W., Jacobs, E. T., and Clark, L. C. Selenium and prostate cancer prevention. *Semin. Urol. Oncol.*, *17*: 91–96, 1999.
39. Green, D. R., and Reed, J. C. Mitochondria and apoptosis. *Science (Wash. DC)*, *281*: 1309–1312, 1998.
40. Muse, K. E., Oberley, T. D., Sempf, J. M., and Oberley, L. W. Immunolocalization of antioxidant enzymes in adult hamster kidney. *Histochem. J.*, *26*: 734–753, 1994.
41. Oberley, L. W., and Buettner, G. R. Role of superoxide dismutase in cancer: a review. *Cancer Res.*, *39*: 1141–1149, 1979.
42. Church, S. L., Grant, J. W., Ridnour, L. A., Oberley, L. W., Swanson, P. E., Meltzer, P. S., and Trent, J. M. Increased manganese superoxide dismutase expression suppresses the malignant phenotype of human melanoma cells. *Proc. Natl. Acad. Sci. USA*, *90*: 3113–3117, 1993.
43. Li, J. J., Oberley, L. W., St Clair, D. K., Ridnour, L. A., and Oberley, T. D. Phenotypic changes induced in human breast cancer cells by overexpression of manganese-containing superoxide dismutase. *Oncogene*, *10*: 1989–2000, 1995.
44. Zhong, W., Oberley, L. W., Oberley, T. D., and St Clair, D. K. Suppression of the malignant phenotype of human glioma cells by overexpression of manganese superoxide dismutase. *Oncogene*, *14*: 481–490, 1997.
45. Liu, R., Oberley, T. D., and Oberley, L. W. Transfection and expression of MnSOD cDNA decreases tumor malignancy of human oral squamous carcinoma SCC-25 cells. *Hum. Gene Ther.*, *8*: 585–595, 1997.
46. Li, N., Oberley, T. D., Oberley, L. W., and Zhong, W. Overexpression of manganese superoxide dismutase in DU145 human prostate carcinoma cells has multiple effects on cell phenotype. *Prostate*, *35*: 221–233, 1998.
47. Rodriguez, A. M., Carrico, P. M., Mazurkiewicz, J. E., and Melendez, J. A. Mitochondrial or cytosolic catalase reverses the MnSOD-dependent inhibition of proliferation by enhancing respiratory chain activity, net ATP production, and decreasing the steady state levels of H₂O₂. *Free Radic. Biol. Med.*, *29*: 801–813, 2000.
48. Manna, S. K., Zhang, H. J., Yan, T., Oberley, L. W., and Aggarwal, B. B. Overexpression of manganese superoxide dismutase suppresses tumor necrosis factor-induced apoptosis and activation of nuclear transcription factor- κ B and activated protein-1. *J. Biol. Chem.*, *273*: 13245–13254, 1998.
49. Chang, B. D., Watanabe, K., Broude, E. V., Fang, J., Poole, J. C., Kalinichenko, T. V., and Roninson, I. B. Effects of p21^{Waf1/Cip1/Sdi1} on cellular gene expression: implications for carcinogenesis, senescence, and age-related diseases. *Proc. Natl. Acad. Sci. USA*, *97*: 4291–4296, 2000.
50. Lu, J., Pei, H., Ip, C., Lisk, D. J., Ganther, H., and Thompson, H. J. Effect on an aqueous extract of selenium-enriched garlic on *in vitro* markers and *in vivo* efficacy in cancer prevention. *Carcinogenesis (Lond.)*, *17*: 1903–1907, 1996.
51. Sinha, R., Said, T. K., and Medina, D. Organic and inorganic selenium compounds inhibit mouse mammary cell growth *in vitro* by different cellular pathways. *Cancer Lett.*, *107*: 277–284, 1996.
52. Bunz, F., Dutriaux, A., Lengauer, C., Waldman, T., Zhou, S., Brown, J. P., Sedivy, J. M., Kinzler, K. W., and Vogelstein, B. Requirement for p53 and p21 to sustain G2 arrest after DNA damage. *Science (Wash. DC)*, *282*: 1497–1501, 1998.
53. Chang, B. D., Xuan, Y., Broude, E. V., Zhu, H., Schott, B., Fang, J., and Roninson, I. B. Role of p53 and p21^{Waf1/Cip1} in senescence-like terminal proliferation arrest induced in human tumor cells by chemotherapeutic drugs. *Oncogene*, *18*: 4808–4818, 1999.
54. Smits, V. A. J., Lompmaker, R., Vallenius, T., Rijkse, G., Makela, T. P., and Medema, R. H. p21 inhibits Thr¹⁶¹ phosphorylation of Cdc2 to enforce the G₂ DNA damage checkpoint. *J. Biol. Chem.*, *275*: 30638–30643, 2000.
55. Shao, Z. M., Alpaugh, M. L., Fontana, J. A., and Barsky, S. H. Genistein inhibits proliferation similarly in estrogen receptor-positive and negative human breast carcinoma cell lines characterized by p21^{Waf1/Cip1} induction, G₂/M arrest, and apoptosis. *J. Cell. Biochem.*, *69*: 391–396, 1998.
56. Choi, Y. H., Lee, W. H., Park, K. Y., and Zhang, L. p53-independent induction of p21 (WAF1/CIP1), reduction of cyclin B1 and G₂/M arrest by the isoflavone genistein in human prostate carcinoma cells. *Jpn. J. Cancer Res.*, *91*: 164–173, 2000.